Clim Dyn (2013) 40:1415–1433
DOI 10.1007/s00382-012-1387-z

Climate simulation over CORDEX Africa domain using the fifth-generation Canadian Regional Climate Model (CRCM5)

Leticia Hernández-Díaz · René Laprise · Laxmi Sushama · Andrey Martynov · Katja Winger · Bernard Dugas

Received: 16 December 2011 / Accepted: 2 May 2012 / Published online: 27 May 2012

Abstract The new fifth-generation Regional Climate Model (CRCM5) was driven by ERA reanalyses for the period 1984–2008 over the African continent following the CORDEX experimental protocol. Overall the model succeeds in reproducing the main features of the geographical distribution and seasonal cycle of temperature and precipitation, the diurnal cycle of precipitation, and the West African Monsoon (WAM). Biases in surface temperature and precipitation are discussed in relation with some circulation defects noted in the simulation. In the African regions near the equator, the model successfully reproduces the double peak of rainfall due to the double passage of the tropical rainbelt, although it better simulates the magnitude and timing of the second peak of precipitation. CRCM5 captures the timing of the monsoon onset for the Sahel region but underestimates the magnitude of precipitation. The simulated diurnal cycle is quite well simulated for all of the regions, but is always somewhat in advance for the timing of rainfall peak. In boreal summer the CRCM5 simulation exhibits a weak cold bias over the Sahara and the maximum temperature is located too far south, resulting in a southward bias in the position of the Saharan Heat Low. The region of maximum ascent in the deep meridional circulation of the Hadley cell is well located in the CRCM5 simulation, but it is somewhat too narrow. The core of the African Easterly Jet is of the right strength and almost at the right height, but it is displayed slightly southward, as a consequence of the southward bias in the position of the Saharan Heat Low and the thermal wind relationship. These biases appear to be germane to the WAM rainfall band being narrower and not moving far enough northward, resulting in a dry bias in the Sahel.

Keywords Regional Climate Modelling · Africa · West African Monsoon · CORDEX

L. Hernández-Díaz (✉) · R. Laprise · A. Martynov · K. Winger
Centre ESCER (Étude et la Simulation du Climat à l'Échelle Régionale), Département des sciences de la Terre et de l'atmosphère, Université du Québec à Montréal (UQAM), C.P. 8888, Succ. Centre-ville, Montreal, QC H3C 3P8, Canada
e-mail: leticia@sca.uqam.ca

L. Sushama
Canada Research Chair in Regional Climate Modelling, Centre ESCER (Étude et la Simulation du Climat à l'Échelle Régionale), Département des sciences de la Terre et de l'atmosphère, Université du Québec à Montréal (UQAM), Montreal, QC, Canada

B. Dugas
Centre ESCER (Étude et la Simulation du Climat à l'Échelle Régionale), Recherche en Prévision Numérique, Environment Canada, Montreal, QC, Canada

1 Introduction

In recent years there has been a surge of international interest in the study of the Africa's climate and in particular the mechanisms explaining the geographic distribution and time variability of rainfall. This is understandable as Africa is not only an exceptionally vulnerable region to climate change "because of the range of predicted impacts and low adaptive capacity" (IPCC AR4 2007), but also to current levels of weather variability. In particular, semiarid regions such as the Sahel are heavily dependent on seasonal rainfall. Severe droughts in this region have led to famine and deaths in the 1970s and 1980s (Druyan 2010). More recently, a severe drought led to a humanitarian crisis affecting 13 million people in the Horn of Africa region (www.redcross.ca). Last but not the least, it has became

clear from the IPCC AR4 (2007) that climate models have difficulties in simulating key elements of present day climate for this continent and hence there is a need to further the understanding of the multiple interactions between the components of the African climate in order to improve climate simulations and projections for this region of the world.

One major element of the African climate is the West African Monsoon (WAM) for which substantial data collection and modelling efforts have been deployed since the African Multidisciplinary Monsoon Analysis (AMMA) project (Redelsperger et al. 2006); to name but a few: the AMMA Model Intercomparison Project (AMMA-MIP; Hourdin et al. 2010), the AMMA land-surface Model Intercomparison Project (ALMIP; Boone et al. 2009), the AMMA "*Couplage de l'Atmosphère Tropicale et du Cycle Hydrologique*" (AMMA-CATCH) project (Lebel et al. 2009), the West African Monsoon Modelling and Evaluation (WAMME) project (Xue et al. 2010; Druyan et al. 2010), and the Ensembles-based Predictions of Climate Change and their Impacts (ENSEMBLES) African project (Paeth et al. 2011).

It is thus not surprisingly that only in the last 2 years, six Journals have dedicated Special Issues to different aspects of the WAM system: Climate Dynamics (2010)—*West African Climate*; Journal of Hydrology (2009)—*Surface processes and water cycle in West Africa studied from the AMMA-observing system*; International Journal of Climatology (2009)—*African Climate and Applications*; Quarterly Journal of the Royal Meteorological Society (2010)—*Advances in understanding atmospheric processes over West Africa through the AMMA field campaign*; Weather and Forecasting (2010)—*West African weather prediction and predictability*; Journal of the Atmospheric Sciences (2010)—*Tropical Cloud Systems and Processes (TCSP) NASA African Monsoon Multidisciplinary Analyses (NAMMA) campaign*.

Africa is also the first target region of the COordinated Regional Climate Downscaling EXperiment (CORDEX; Giorgi et al. 2009; http://cordex.dmi.dk/joomla/), an initiative of the World Climate Research Programme (WCRP; http://www.wcrp-climate.org/) aiming at regional climate modelling evaluation and improvement. CORDEX also provides an opportunity to test the model outside its native region, as strongly recommended by the GEWEX *Transferability Working Group* (TWG; http://rcmlab.agron.iastate.edu/twg/regional.html) and *Inter-Continental Scale Experiments (CSE) transferability Study* (ICTS; http://www.clm-community.eu/index.php?menuid=1&reporeid=25; Takle et al. 2007).

The diversity of climate regimes over Africa, covering tropical and mid-latitudes in both hemispheres, represents a considerable challenge for climate models (IPCC AR4 2007). A recent analysis of simulated precipitation climatology from the first set of CORDEX-Africa ensemble simulations can be found in a recent paper by Nikulin et al. (2012).

It is in this context that the new fifth-generation Canadian Regional Climate Model (CRCM5) has been applied to CORDEX-Africa, which appears a good opportunity to study the model performance in simulating the key elements of the African climate, including the WAM. The aim of this paper is to describe CRCM5 and to show its skill in simulating present climate over a domain outside its "native" region as recommended by the WCRP: the CORDEX-Africa domain. The main features of CRCM5 are described in Sect. 2. Section 3 follows with a description of the configuration of the model simulations and the data used as reference, and Sect. 4 with the presentation and discussion of results including the annual and diurnal cycle of precipitation over the continent and the simulated WAM climatology. Conclusions are given in Sect. 5.

2 Model description

CRCM5 uses the dynamical core and several subgrid-scale physical parameterisation modules of the Canadian Global Environment Multiscale (GEM) model, in a limited-area model (LAM) configuration (Zadra et al. 2008).

The GEM model was developed for Numerical Weather Prediction (NWP) at the *Division de Recherche en Prévision Numérique* (RPN) of the Meteorological Service of Canada (MSC; Côté et al. 1998a, b). GEM uses a two-time-level (almost) fully implicit semi-Lagrangian marching scheme, with slight off-centring to reduce the spurious response to orographic forcing (Tanguay et al. 1992). In the horizontal the discretisation uses an Arakawa staggered C-grid and in the vertical a hybrid terrain-following hydrostatic-pressure coordinate (Laprise 1992). Initially GEM offered two configurations within a single global modelling system based on a latitude-longitude grid, with optional rotation of the poles: a regular latitude-longitude version and a variable-resolution stretched-grid version. Shortly after a fully elastic non-hydrostatic option was implemented (Yeh et al. 2002), the model was adapted for distributed-memory massively parallel computers, and a nested LAM option was also developed.

The nested LAM version of GEM was adopted for the developmental version of the CRCM5 that was initiated more than a decade ago through a collaboration established between ESCER/UQAM, RPN/MSC and the OURANOS Consortium. In CRCM5 one-way nesting is implemented following Davies (1976): over a 10 grid-point "sponge" ribbon around the domain perimeter, the simulated atmospheric variables are gradually relaxed towards the

imposed lateral boundary conditions for horizontal winds, temperature, specific humidity and surface pressure fields. In addition a 10 grid-point "halo" region is added around the domain in order to provide upstream values for the semi-Lagrangian transport scheme; there are no calculations performed in this halo region, other than interpolating for the upstream values. An option also exists for weakly nudging the large scales within the interior of the domain, similar to earlier versions of CRCM (e.g. Biner et al. 2000; Riette and Caya 2002; Laprise 2008), although this option will not be activated for the experiments reported here. However the temperature at the uppermost level of CRCM5 is forced to the value of the driving data.

GEM supports a diversity of subgrid-scale physical parameterisations, depending upon the application and resolution. CRCM5 employs a mixture of the parameterisation modules of GEM in its so-called "meso global" and "regional" versions (based on MSC's source-code libraries 3.3.3 for the Dynamics and 5.0.4 for the Physics). GEM is used for 3- to 5-day forecasts, seasonal prediction and AMIP-type simulations (e.g. Fox-Rabinovitz et al. 2006). Physical parameterisations include the Kain and Fritsch (1990) deep-convection scheme, the Kuo-transient scheme for shallow convection (Kuo 1965; Bélair et al. 2005), the Sundqvist scheme for large-scale condensation (Sundqvist et al. 1989), the correlated-K scheme for solar and terrestrial radiations (Li and Barker 2005), a subgrid-scale mountain gravity-wave drag (McFarlane 1987) and low-level orographic blocking (Zadra et al. 2003), a turbulent kinetic energy closure in the planetary boundary layer and vertical diffusion (Benoit et al. 1989; Delage and Girard 1992; Delage 1997), and a weak ∇^6 lateral diffusion.

Aerosols are not yet implemented in this version of the model. For CRCM5 the usual ISBA land-surface scheme of GEM has been changed for the Canadian LAnd Surface Scheme (CLASS; Verseghy 2000, 2008) in its most recent version, CLASS 3.5, that allows for a detailed representation of vegetation, land-surface types, organic soil and a flexible number of layers. For these simulations three layers are used in CLASS 3.5, with depths of 10, 25 and 375 cm. The standard CLASS distributions of sand and clay fields as well as the bare soil albedo values were replaced by data from the ECOCLIMAP database (Masson et al. 2003). An interactive lake module is implemented in CRCM5; for the simulations reported here the FLake model was used; see Martynov et al. (2010, 2012) for more details.

Several research projects have been carried out using developmental versions of CRCM5 (e.g., Takle et al. 2007; Caron et al. 2010; Caron and Jones 2011; Paquin-Ricard et al. 2010; He et al. 2010; Šeparović et al. 2011; Diaconescu et al. 2011). CORDEX, with its focal region over Africa, hence provides an opportunity to thoroughly test CRCM5 outside its "native" region, as strongly recommended by the WCRP and GEWEX.

3 Simulation configuration

CRCM5 was integrated over the African domain recommended by CORDEX (Fig. 1) with a horizontal grid spacing of 0.44° and a 20-min timestep for the period 1984–2008. The initial 5 years were discarded to allow spin-up of land-surface fields, and the results were analysed for the CORDEX period 1989–2008. The computational domain has 216 × 221 grid points, including the sponge zone. In the vertical, 56 levels were used with the top level near 10 hPa and the lowest level at $0.996 \times p_s$ where p_s is the surface pressure. For diagnostic analysis the simulated fields were interpolated to 12 pressure levels (1,000, 925, 850, 700, 600, 500, 400, 300, 250, 200, 150 and 100 hPa), and most variables were archived at three hourly intervals, except precipitation and surface fluxes that were cumulated and archived at hourly intervals.

A ∇^6 lateral diffusion is applied to atmospheric variables with a constant chosen such as to remove 4% of the amplitude of shortest resolved scales at every time step. Off-centring in the time-averaging along the trajectory for the implicit semi-Lagrangian scheme uses weights of 0.55 and 0.45 for the future/downstream and past/upstream contributions, respectively.

The atmospheric lateral boundary conditions (LBC), as well as sea-surface temperatures (SSTs), for the CRCM5 simulations came from the European Centre for Medium-range Weather Forecasting (ECMWF) gridded reanalyses (ERA; Simmons et al. 2007, Uppala et al. 2008), available to us at a resolution of 2.0° at 6 hourly intervals on 22 pressure levels (1,000, 975, 950, 925, 900, 850, 800, 700, 600, 500, 400, 300, 250, 200, 150, 100, 70, 50, 30, 20, 15 and 10 hPa). For the spin-up period (1984–1988), LBCs and SSTs came from ERA-40 reanalyses, while for the main CORDEX study period (1989–2008), the ERA-Interim data provided the driving conditions.

The simulations are compared to available observational datasets such as CRU (Climate Research Unit version 3.1 from 1901 to 2009; Mitchell and Jones 2005; Mitchell et al. 2004) and UDEL (University of Delaware version 2.01: 1901–2008; Legates and Willmott 1990a, b; Willmott et al. 1998) gridded analyses at 0.5° spatial and monthly temporal resolution, GPCP (Global Precipitation Climatology Project; Adler et al. 2003), TRMM (Tropical Rainfall Measuring Mission; Huffman et al. 2007), and the driving ERA-Interim reanalyses. The GPCP precipitation datasets are estimations of rainfall resulting from a combination of rain-gauge stations and satellite geostationary and low-orbit infrared, passive microwave and sounding

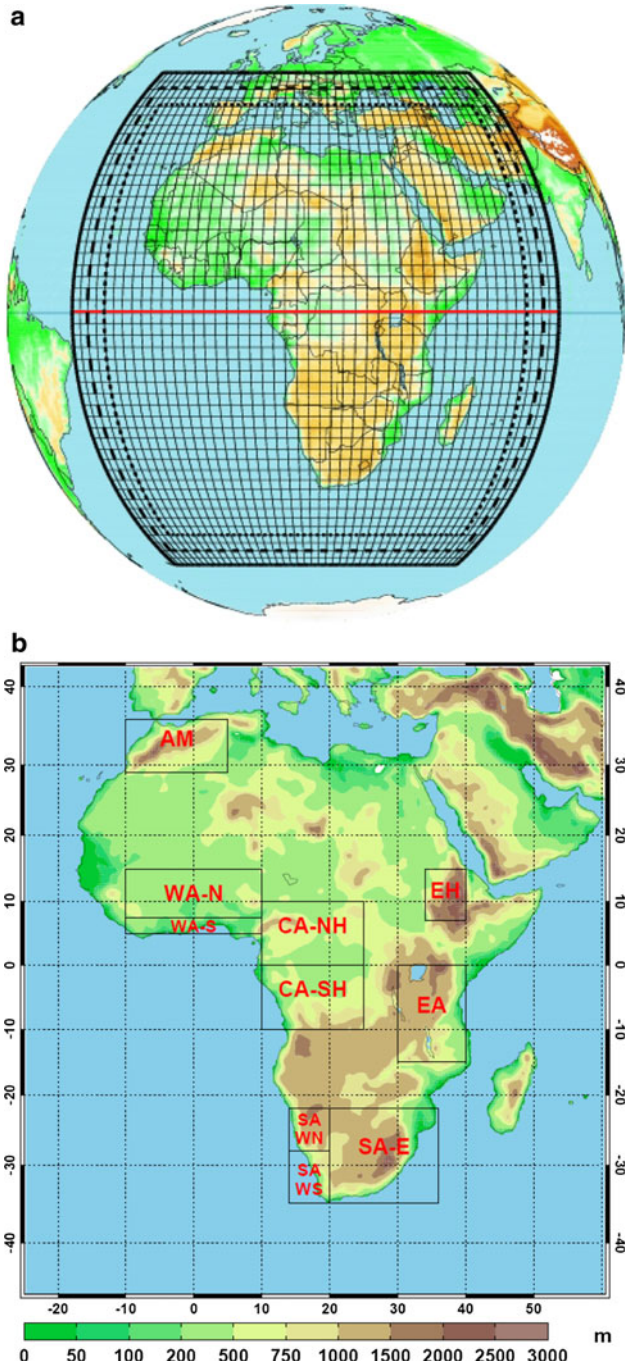

Fig. 1 **a** CRCM5 CORDEX-Africa simulation domain, with only every 5th *grid box* displayed. **b** The *different regions* within the African domain taken from http://www.smhi.se/forskning/forskningsomraden/klimatforskning/1.11299

observations; we used here the 1° daily dataset available from 1997 (Huffman et al. 2001). The TRMM dataset is based on a combination of multiple satellite-rainfall estimates and gauge analyses at a resolution of 0.25° at 3 hourly (3B42) and monthly intervals (3B43), covering the period from 1998 to present (Huffman et al. 2007); the model-simulated diurnal cycle of rainfall for several regions will be compared to those obtained from the TRMM 3B42 dataset, and the TRMM 3B43 will be used to compare the model-simulated annual cycle over selected regions and the seasonal means maps.

4 Results

4.1 Seasonal mean climatology

The seasonal mean 2-m temperature from CRU gridded analysis, as well as ERA-Interim reanalyses and CRCM5 simulation during the periods January–February–March (JFM) and July–August-September (JAS) are shown in Fig. 2, along with the simulation bias (CRCM5 minus Observations). The periods JFM and JAS will henceforth be referred to as the austral and boreal summers, since these periods match best with the migration of the tropical rainbelt over tropical Africa. The simulation reproduces the overall features of geographical and seasonal temperature distribution. Compared to CRU, there is however a cold bias in the CRCM5 simulation in JFM (Fig. 2a) over most of the domain south of the equator, as well over the West Africa region and the Saudi Arabia peninsula. At the same time, there is a warm bias near the border between the Central African Republic and the Democratic Republic (DR) of Congo. The cold bias appears larger compared to UDEL dataset but is smaller when compared to ERA. The warm bias in Democratic Republic (DR) of Congo is on the contrary larger when compared to ERA-Interim.

In JAS (Fig. 2b), CRCM5 exhibit a cold bias over the East Africa Highlands, the elevated terrains of Ethiopia and Sudan, eastern Madagascar, the NW of Saudi Arabia, and over the coastal countries of the Gulf of Guinea when compared to CRU and UDEL datasets. On the other hand, the model is warmer than CRU in regions such as the Sahara, the apparent warm bias reaching up to 2° in regions such as the southern Congo basin and Oman. In fact, as can be seen when comparing with ERA-Interim reanalyses or UDEL dataset, the CRCM5 simulation has a weak cold bias over the Sahara rather than a warm bias as would imply the CRU data. We hypothesise that due to the paucity of observations over the Sahara the CRU gridded analysis misses the hottest pool, with temperatures exceeding 36° on average over northern Mali and southern Algeria according to ERA-Interim and UDEL.

In conclusion, albeit with some biases, the CRCM5 simulation succeeds in reproducing the detailed geographical distribution and seasonal variations of temperatures. As a matter of fact Sylla et al. (2010), in their simulation of the African climate using a regional climate model, found that a temperature bias of ±2° is in the range

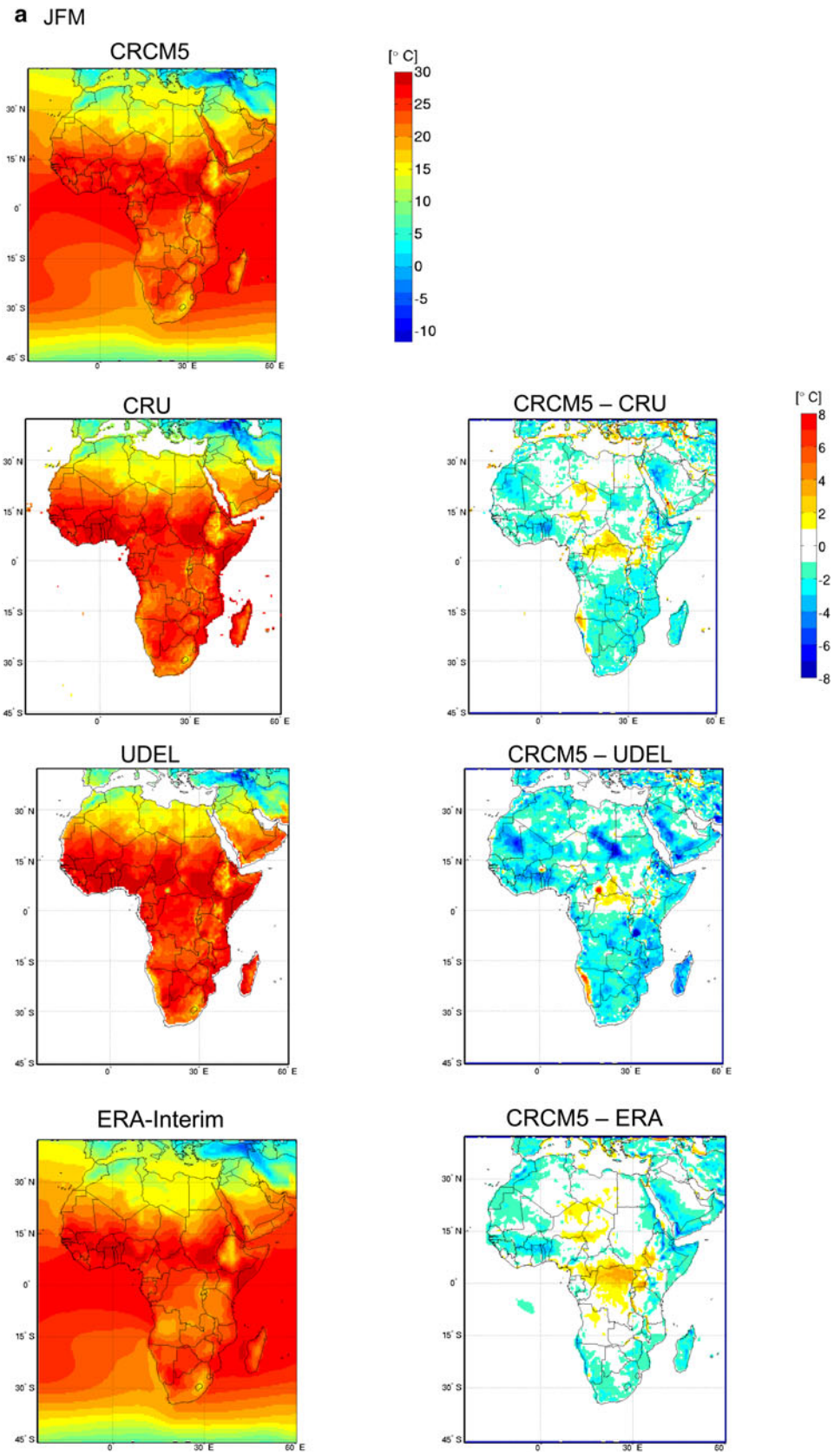

Fig. 2 Mean (1989–2008) 2-m temperature in **a** JFM and **b** JAS seasons from CRCM5, CRU, UDEL, ERA-Interim (*left column*) and the difference CRCM5 minus OBS (*right column*)

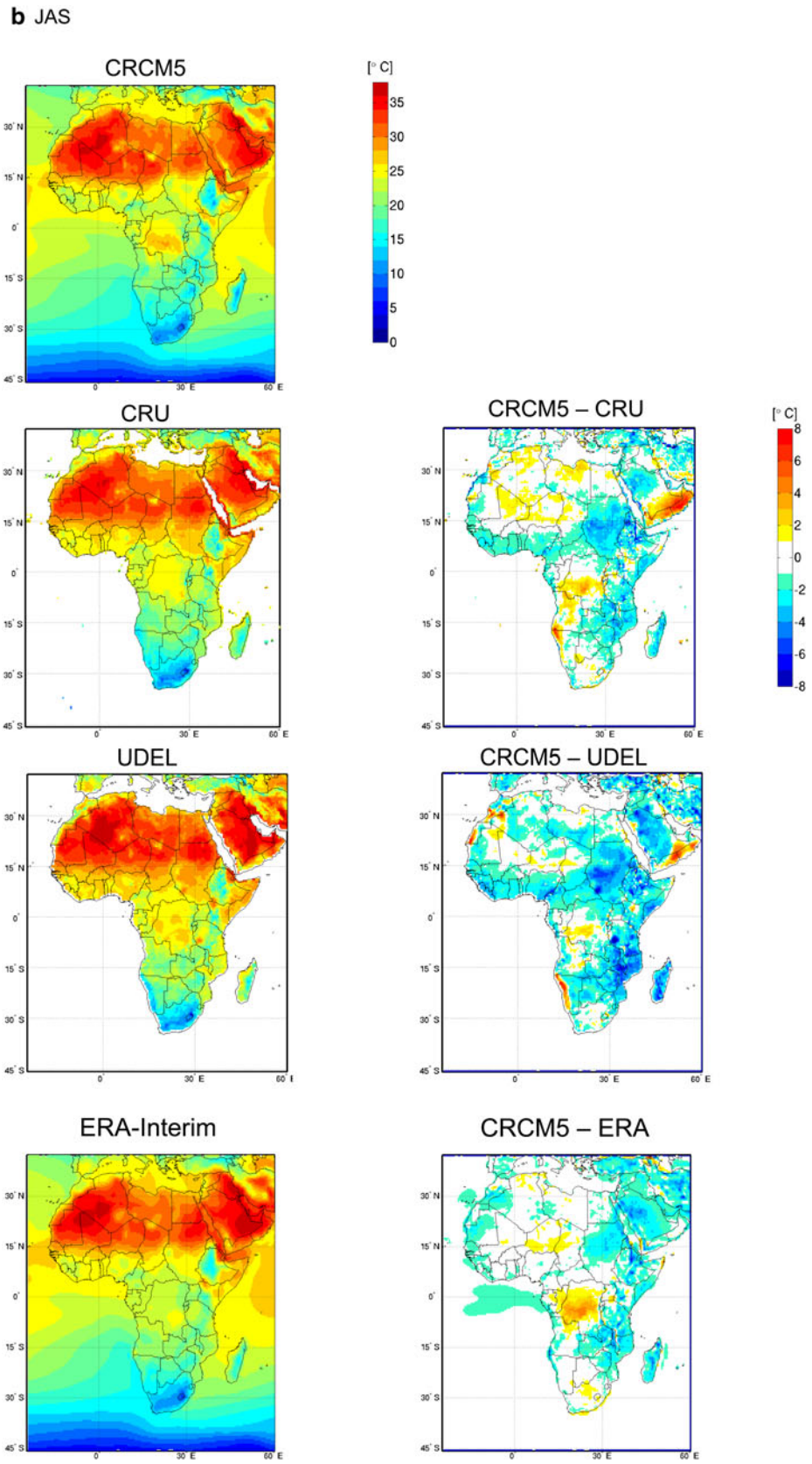

Fig. 2 continued

of state-of-the-art regional climate models. What constitutes the best reference dataset for simulation validation remains an open issue in regions with poor observational coverage.

CRCM5-simulated precipitation fields for JFM and JAS are compared to those from GPCP, TRMM, CRU and UDEL datasets in Fig. 3. As most of the African continent lies within the tropics, the seasonal migration of the tropical rainbelt that regulates the alternation of wet and dry seasons, is the principal characteristic of precipitation over the continent. Furthermore, small shifts in the position of the rainbelt can result in large local changes in precipitation; this has a direct impact upon water resources and agriculture in the semiarid regions of the continent, such as the Sahel. There are also regions on the northern and southern limits of the continent with winter rainfall regimes that are governed by the passage of mid-latitude fronts. The wettest regions in Africa are those of the equatorial, tropical rainforest climate type, where there is rain throughout the year, with two peak periods corresponding to the double passage of the tropical rainbelt. The driest regions are those of the desert climate type, such as those of the Sahara, Kalahari and Somali deserts, where there is very little precipitation.

During the period of high sun in austral Africa (JFM), the tropical rainbelt is at its southernmost position (Fig. 3a). The bulk of precipitation over the continent is thus mainly circumscribed to the regions south of the equator. Rainfall peaks of 8–12 mm/day are found in Mozambique, Malawi, Zambia and Gabon, but the most intense are found in the east and northwest coasts of Madagascar with more than 20 mm/day. The model simulation compares well with observational datasets. In fact for some regions it can be argued that the model-simulated precipitation may be more realistic than the 1° GPCP and even the 0.5° gridded datasets; this is the case for the Gabon, DR of Congo and Madagascar regions. This may be the result of the CRCM5 higher resolution that allows a fairly realistic description of physiographic effects such as lowlands, escarpments and plateaus that characterise these regions. For example, according to the Historical and Meteorological Data Center (HMDC) for Madagascar (NOAA Central Library, http://docs.lib.noaa.gov/rescue/data_rescue_madagascar.html), the lowlands along the southern and western coasts of Madagascar receive 400–800 mm of annual rainfall, while most of the mountainous east coast, as well as a small region in the northwest, have an annual rainfall over 2,000 mm. Precipitation in the central plateau has intermediate values: 1,000–1,500 mm according to HMDC. Being exposed to the moisture-laden trade winds, the east coast is wet for much of the year, while the rest of the island receives most of the rainfall between November and March (HMDC). CRCM5 and TRMM reproduce this pattern while the coarser mesh GPCP analysis misses it. GPCP also misses the rainfall peak in the highlands of Gabon and the DR of Congo. It must be mentioned also that in the southeast part of the domain, near the boundary, there is an overestimation of rainfall over the ocean, especially in this season. The reasons for this bias are unknown at the moment, but we hypothesize as does Nikulin et al. (2012) that this may be related to the representation of convection in the model boundary relaxation zone.

In AMJ (not shown), the tropical rainbelt begins its northward displacement and is located near the equator. This is the beginning of the rainy season for the Guinean coastal region and the first rainfall onset of the West African Monsoon (WAM). Rainfall peaks are still present over the east coast of Madagascar and the highlands regions of Gabon. The CRCM5 simulates rainfall peaks of 8–12 mm/day in the Guinea coastal region, which do not appear in GPCP.

During the boreal summer (JAS), the tropical rainbelt moves to its northernmost location (Fig. 3b) and so does the rainfall peak of the WAM, which is located around 10°N. This is the second rainfall onset of the WAM and the beginning of the rainy season for the Sahel. Precipitation is mostly confined between the equator and around 15°N; the width of the rain band is slightly narrower in the model than in all of the observation datasets, resulting in a dry bias in the Sahel and the DR of Congo as well as in the Gulf of Guinea. CRCM5 and GPCP as well as CRU and UDEL show 3 maxima of precipitation (from 8 to 12 mm/day and for some up to 24 mm/day) over the highlands of Guinea, near the Nigeria—Cameroon border and Ethiopia; the CRCM5 has higher values than the gridded analyses in those regions. TRMM shows an underestimation of rainfall in the Ethiopian Highlands region when compared to the other datasets as well as to CRCM5. In the southern hemisphere, away from the equator, the only African regions to receive non-negligible rain during this season are the east coast of Madagascar and some parts of Mozambique; in Madagascar the CRCM5 simulates a sharp line of precipitation with peak values higher than in GPCP and the other datasets, and in Mozambique all datasets fail to show any substantial precipitation at all.

In OND (not shown), the tropical rainbelt is on its journey southward and so does the spatial pattern of precipitation over the continent.

4.2 Annual cycle of precipitation

Figure 4 shows the mean annual cycle of precipitation for some of the African-CORDEX regions as displayed in Fig. 1b. For each region are shown the CRCM5 simulation, as well as the CRU and GPCP data sets for the period

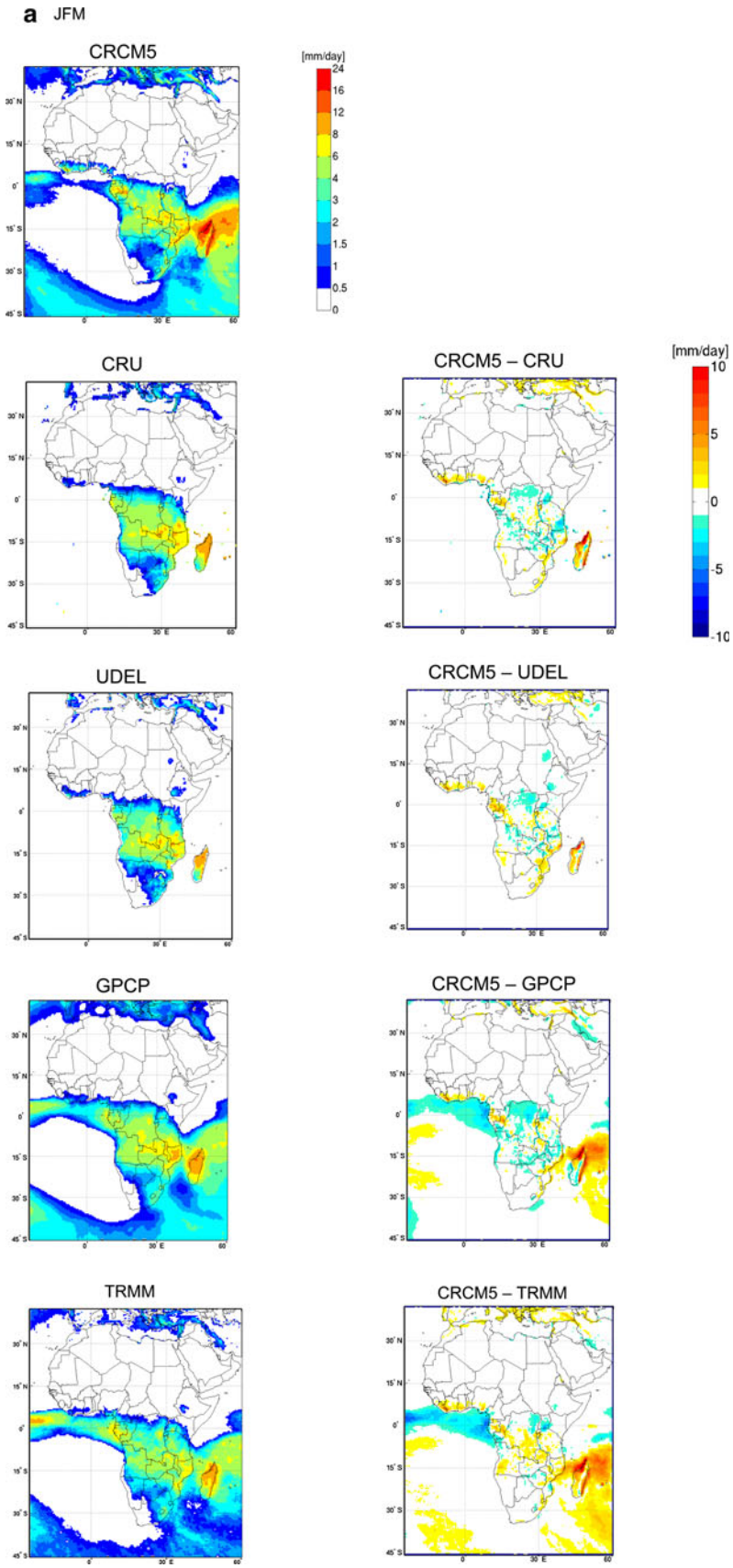

Fig. 3 Mean (1997–2008) precipitation in **a** JFM and **b** JAS seasons from CRCM5, CRU, UDEL, GPCP and TRMM (*left*) and the difference CRCM5 minus OBS (*right*). TRMM period is (1998–2008)

Fig. 3 continued

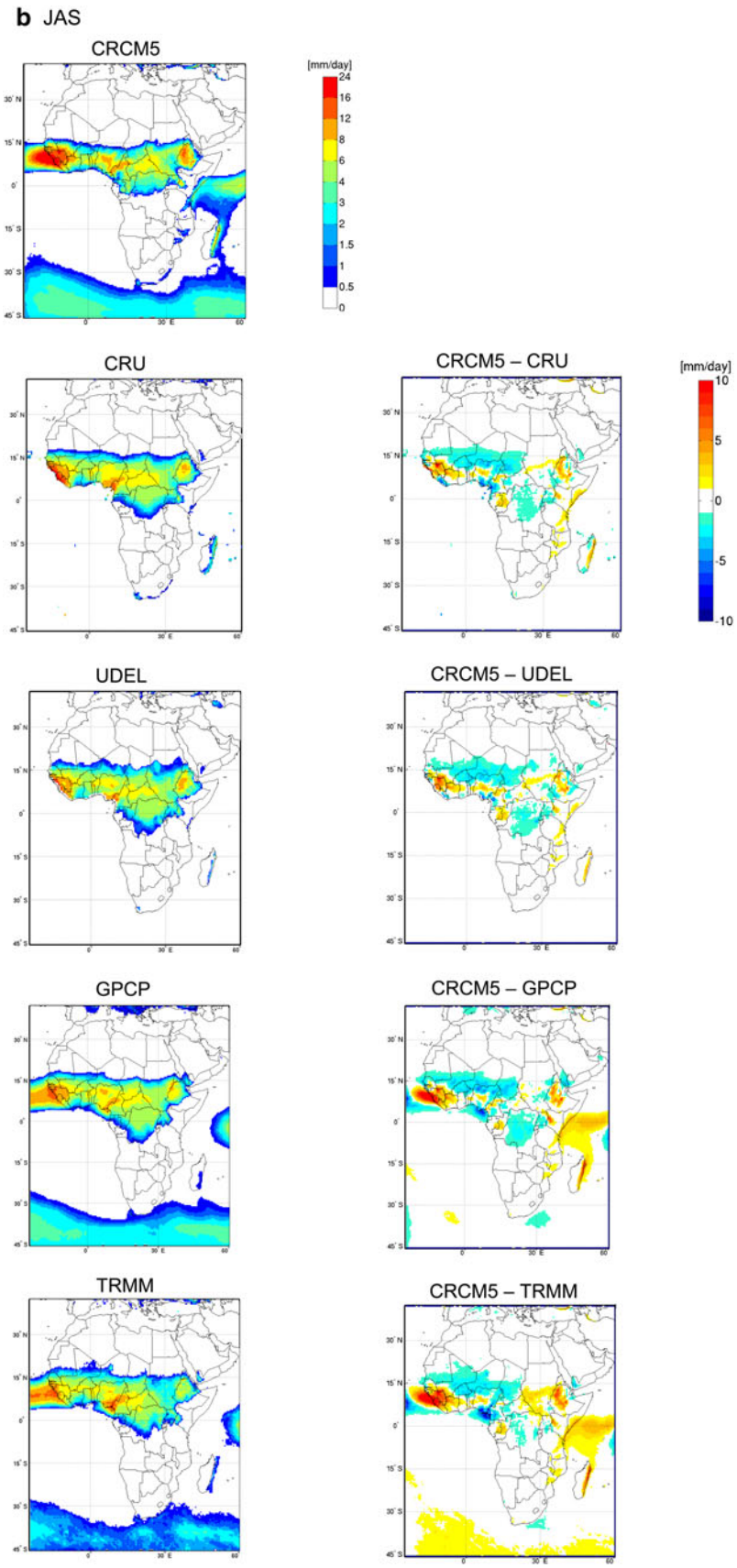

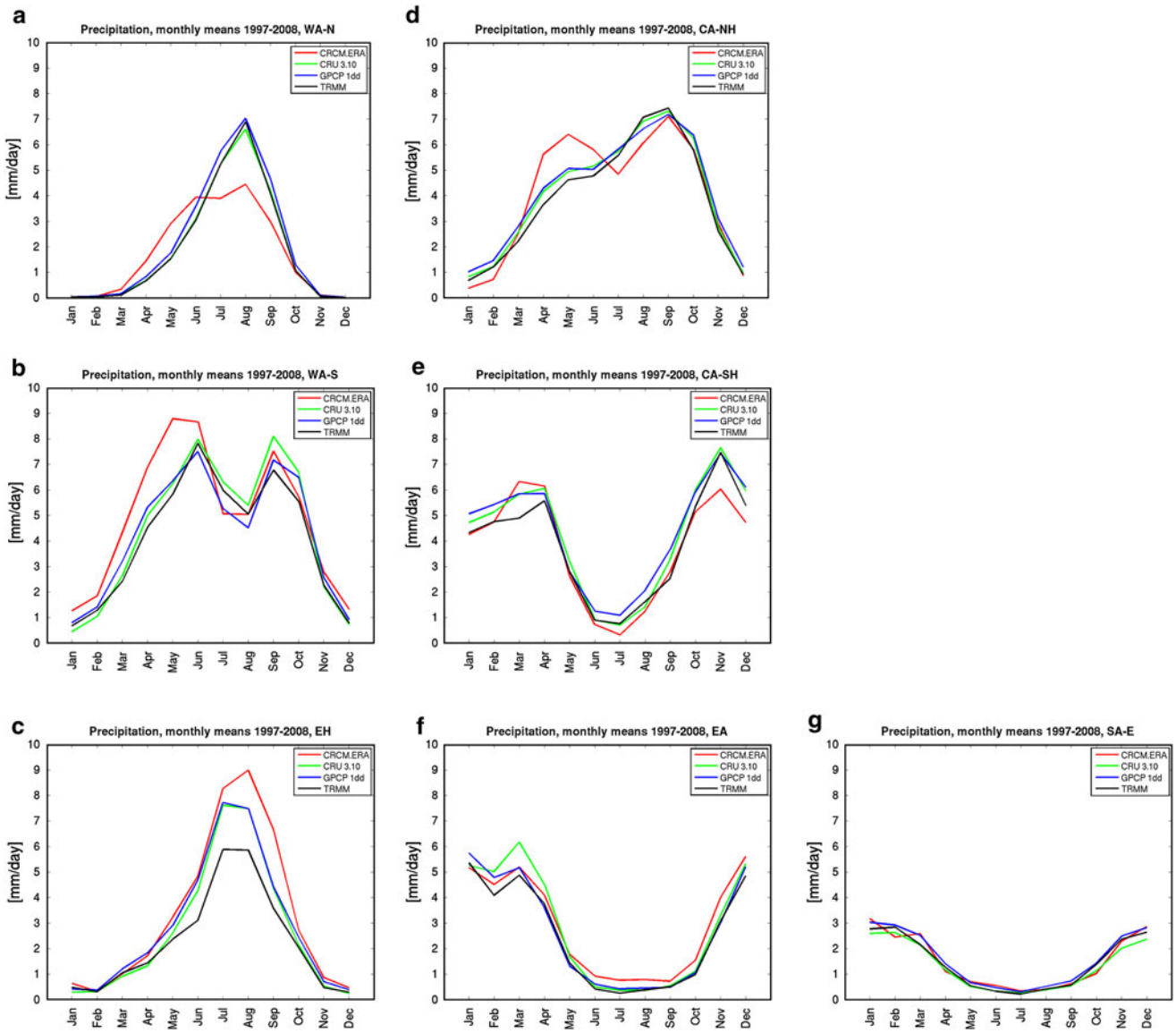

Fig. 4 Mean (1997–2008) annual cycle of precipitation (mm/day) from CRCM5 (*red*), CRU (*green*), GPCP (*blue*) and TRMM (*black*) for regions of the African CORDEX domain: **a** West Africa—North, **b** West Africa—South, **c** Ethiopian Highlands, **d** Central Africa—Northern Hemisphere, **e** Central Africa—Southern Hemisphere, **f** East Africa, **g** South Africa—East. TRMM period is (1998–2008)

1997–2008, and the TRMM dataset for the period 1998 to 2008. In the regions near the equator (Fig. 4b, d, e) there is double peak of rainfall due to the double passage of the tropical rainbelt. The simulations and the observations are very close for the Central Africa—North (Fig. 4d) and South (Fig. 4e) regions, although the bimodal character of precipitation is more visible in the simulation than in the observations in the case of the Central Africa—North region (Fig. 4d). Over the West Africa—South region (Fig. 4b), the observations exhibit two pronounced rainfall peaks: the coastal monsoon onset at the end of May, which is the first rainy season for this region, and the second one when the tropical rainbelt is in its southern migration towards its boreal winter location. The CRCM5 simulation agrees better with the observations in the magnitude and timing of the second peak of precipitation. For the first rainfall peak, the simulation overestimates the magnitude and the monsoon onset is somewhat too early.

The West Africa—North region (Fig. 4a), which includes the Sahel, is characterised by a single peak of precipitation occurring in August when the monsoon reaches its farthest northward position. The peak precipitation intensity is somewhat deficient in the simulation, although simulated precipitation is somewhat excessive in the April–May period.

Over the Ethiopian Highlands region (Fig. 4c), maximum precipitation occurs around July–August. The simulation is able to reproduce accurately the gradual rise of

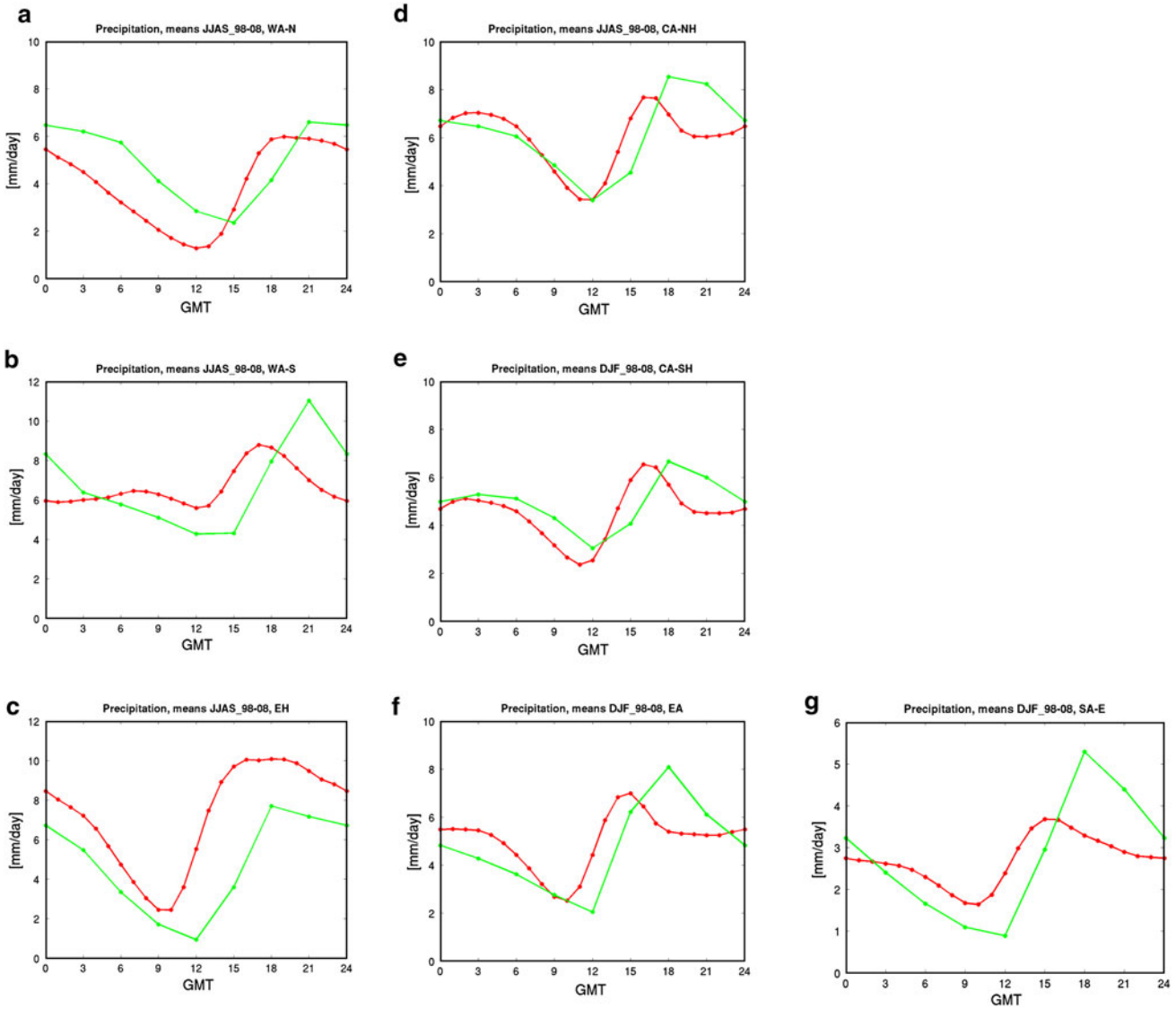

Fig. 5 Mean (1998–2008) diurnal cycle of precipitation from TRMM dataset (*green*) and CRCM5 simulation (*red*) over regions of the African CORDEX domain: **a** West Africa—North, **b** West Africa—South, **c** Ethiopian Highlands, **d** Central Africa—Northern Hemisphere, **e** Central Africa—Southern Hemisphere, **f** East Africa, **g** South Africa—East

precipitation from January to July, but the simulated peak is overestimated and precipitation is excessive till September. In the East Africa Highlands (Fig. 4f) maximum precipitation occurs around January-March; in the simulation there is a little overestimation of rainfall during the dry season and before the time of the peak. Over the South Africa—East region (Fig. 4g), the annual cycle of precipitation is similar to that of the East Africa Highlands, but weaker; the simulation successfully captures the timing and magnitude of the precipitation cycle.

4.3 Diurnal cycle of precipitation

The diurnal cycle of precipitation is another good metric for assessing the skill of climate model simulations because of the multiple dynamical, thermal and radiative processes that are associated with it (Ploshay and Lau 2010). As stated by Yang and Slingo (2001): "The simulation of the amplitude and phase of the diurnal cycle provides an ideal test bed for model parameterizations and for the representation of the interactions between the surface, the boundary layer, and the free atmosphere."

The main feature of the diurnal cycle of precipitation in the tropics is a late afternoon—evening maxima over land (Dai et al. 2007, Yang and Slingo 2001). Using the 3 hourly TRMM observational dataset as reference, the mean diurnal cycle of simulated precipitation for the period 1998–2008 were plotted for some of the Africa CORDEX regions shown in Fig. 1b, during the season of their

maximum precipitation. For the regions with two rainy seasons, only one is shown but the other is commented upon if necessary. As can be seen from the TRMM data in Fig. 5 most regions have a late afternoon maximum of precipitation, around 18 GMT, while the West Africa ones (Fig. 5a, b) exhibit a later occurrence of their maximum, around 21 h GMT. This would be related to the fact that in West Africa most of the precipitation comes from mesoscale convective systems triggered by the orography and elevated daytime heating (Hodges and Thorncroft 1997; Yang and Slingo 2001) which are typically initiated between 17 and 18 h (Local Time) but for which the maximum of precipitation occurs at the mature stage, later in the night (McGarry and Reed 1978; Hodges and Thorncroft 1997; Yang and Slingo 2001; Nikulin et al. 2012).

Figure 5 shows that overall CRCM5-simulated diurnal cycle of precipitation agrees with TRMM observations in phase and amplitude, albeit with some differences from one region to another. The model does particularly well in the Central Africa North (Fig. 5d) and South (Fig. 5e) regions, although the timing of maximum rainfall in CRCM5 is somewhat earlier than observed. This difference in the time of maximum rainfall is still more pronounced in the first rainy season (AMJ) for the Central Africa—North region (not shown), in which case the simulation also gives higher rates of precipitation. Concerning the Central Africa—South region the diurnal cycle of both seasons (FMA, not shown and OND) is very similar. In the Ethiopian Highlands region (Fig. 5c) there is an overestimation of the rate of precipitation in the simulation. On the other hand, in the East Africa Highlands (Fig. 5f), there is a little overestimation of the rate of rainfall before the time of the maxima but an underestimation afterwards. This is also the case of the South Africa—East region (Fig. 5g). The timing of the simulated rainfall peak is too early for these two regions. In the West Africa South (Fig. 5b) region the peak of simulated rainfall occurs earlier than observed for the two rainy seasons (AMJ, not shown, and ASO), but the model is better in reproducing the diurnal cycle of the ASO peak although the magnitude of the rainfall peak is somewhat underestimated. On the other hand, the results for the West Africa North (Fig. 5a) region show a very good amplitude of the simulated diurnal cycle, but its timing is in advance by two to three hours.

Although the simulated diurnal cycle is not perfect, being always in advance for the timing of rainfall peak, we can say that CRCM5 reproduces the pattern of the observed diurnal cycle most of the time. In their comparison of several regional models over Africa, Nikulin et al. (2012) remarked that CRCM5 best reproduced the diurnal cycle of precipitation.

4.4 West African Monsoon climatology

A detailed analysis of the West Africa—North region is presented in this section. Figure 4a showed that CRCM5 captures the timing of the monsoon onset for the region but underestimates the magnitude of precipitation. This is clearly reflected in the Hovmöller-type diagrams presented in Fig. 6. This figure shows time-latitude cross-sections of daily precipitation from GPCP as well as from the CRCM5 simulation, averaged over 10°W–10°E for the period 1997–2008. A 31-day moving average has been applied to remove high-frequency variability. The simulation captures to some extent the evolution of the monsoonal rainfall. However in the simulation the first peak occurring around day 150 is excessive compared to that of GPCP and the northern limit of precipitation (as defined by the 1 mm/day contour) is located around 15°N while it is found at almost 20°N in GPCP; CRCM5 has thus a dry bias in the Sahel.

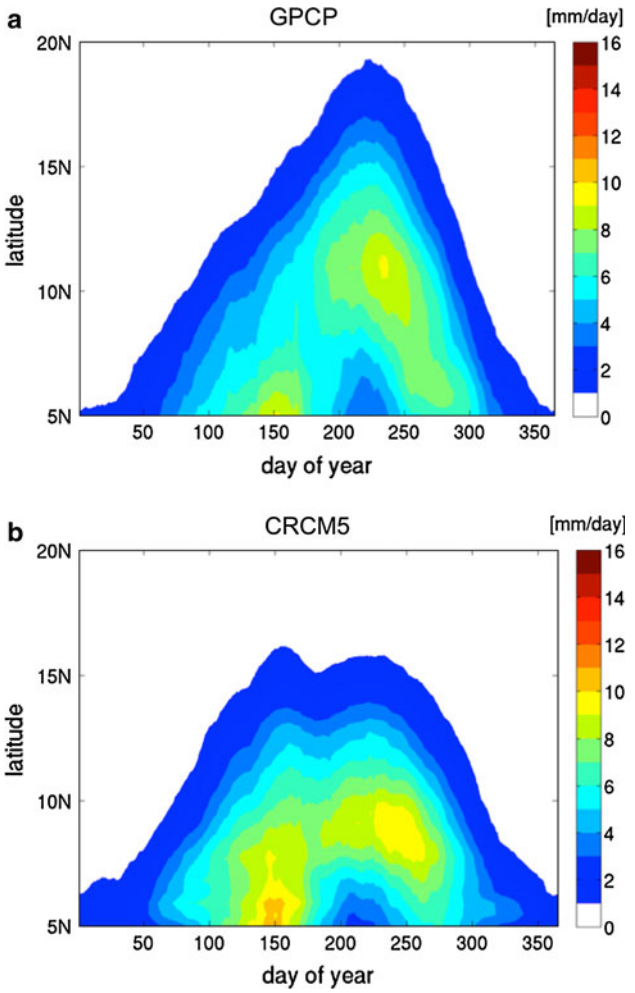

Fig. 6 Mean (1997–2008) annual cycle of precipitation (mm/day) over West Africa from **a** GPCP 1DD values and **b** CRCM5 simulation, averaged over 10°W–10°E. A 31-day moving average has been applied to remove high-frequency variability

Despite the model dry bias in the Sahel that is still present, the intensity of the rainfall peaks in the Hovmöller diagram matches better with those of the TRMM dataset shown in Fig. 6 of Nikulin et al. (2012).

Figure 7 (panels a and b) shows maps with a superposition of the 2-m temperature (colours), mean sea level pressure (MSLP, contours) and low-level wind vectors (arrows) during the boreal summer, for the ERA-Interim data (Fig. 7a) and CRCM5 simulation (Fig. 7b). The contrast between the hot Sahara and the colder equatorial Atlantic Ocean in this season can be clearly seen. The large-scale pressure gradient between the two regions gives rise to a southerly flow from the ocean to the land. The zone where the humid and cooler southwesterly (monsoonal) flow meets the dry and hot northeasterly (Harmattan) flow lies in the southern fringe of the West African Heat Low (WAHL), or Saharan Heat Low (SHL) as it is often named for its summer position over the Sahara region (e.g., Lavaysse et al. 2009). The surface position of this lower tropospheric convergence is called the Inter-Tropical Front (ITF) or Inter-Tropical Discontinuity (ITD; Lavaysse et al. 2009). In the reanalyses, it is located as far inland as 20–22°N.

The CRCM5 simulation reproduces the overall features present in the ERA-Interim analyses, but with some deficiencies. In the CRCM5 simulation, the maximum temperatures located in the Sahara (northern Mali and southern Algeria) are not high enough, but the secondary maximum located further southeast in Niger and Chad is somewhat too high. The resulting southward shift of the position of maximum surface temperature induces a southward bias in the position of the SHL, as can be seen in Fig. 7c, where the bias of mean sea-level pressure (MSLP) is shown. As a consequence, the monsoonal flow does not extend far enough to the north, and this could be the reason why the summer monsoonal rainfall in the Sahel region is much too weak in the simulation, as we shall see below.

In order to better analyse the WAM, Fig. 8 zooms on the region between 10°W–10°E and 10°S–35°N, over the period 1997–2008, as represented by ERA-Interim (top) and the CRCM5 simulation (bottom). The left panels present maps with a superposition of the fields of 2 m-temperature (colours), 925-hPa horizontal wind vectors (arrows) and precipitation (contours); the right panels present vertical cross-sections with a superposition of vertical velocity (mm/s) plotted in colours and arrows displaying vectors combining vertical (mm/s) and meridional (m/s) velocity components, and a line curve showing the GPCP precipitation intensity. Such composite diagram allows grasping at a glance some of the key dynamical processes associated with the WAM and to evaluate the skill of the model in simulating the WAM.

The most striking feature when looking to the left panels of Fig. 8 is the difference in surface temperature between the model and reanalysis in this region. Compared to the analyses the simulation shows a weaker surface temperature gradient and a narrower precipitation belt that is located further south. Also noticeable is the fact that the monsoonal winds barely reach 15°N in the simulation whereas in the reanalysis they reach up to 20°N; not surprisingly, the northern precipitation isoline of 1 mm/day has a similar southward displacement bias in the simulation.

As noted before, in the simulation the Sahara is not warm enough and the warmest part is located too far south and east. As a consequence, the heat low that develops in summer over this region is displaced to the south. This implies a southward displacement of the zone of convergence of the humid and cooler south-westerly monsoonal flow with the hot and dry north-easterly Harmattan flow. As a result, the vertical ascent associated with the low-level convergence of the Harmattan and monsoonal winds is located too far south in the CRCM5 simulation with respect to the reanalysis, as can be seen in the right panel of Fig. 8. This region of shallow ascent corresponds to the shallow meridional circulation (SMC) cell from the surface to the mid-troposphere (Nicholson 2009; Thorncroft et al. 2011) associated to the Saharan Heat Low. As can be seen in Fig. 8, the maximum ascent is located north of 20°N in the reanalysis while in the simulation it is found farther south (between 15°N and 20°N).

On the other hand, the deep meridional circulation associated with the Hadley cell (Nicholson 2009; Thorncroft et al. 2011) is represented by a column of rising air centred around 10°N, but it is narrower in the simulation than in the reanalysis. This region of strong ascent is responsible for the bulk of precipitation; this is the tropical rainbelt (Nicholson 2008) and maximum rainfall coincides with maximum ascent. The dry bias of the CRCM5 simulations in the Sahel is in accordance with the southward bias in the position of the northern edge of this column of rising air, as well as the southward bias in the location of the SMC of the WAHL. However, the region of maximum ascent and rainfall in CRCM5 is collocated with that in ERA-Interim.

Finally, there is also a region of shallow ascent located around 5°N which corresponds to the coastal meridional sea-breeze circulation. This feature is less developed in the simulation than in the reanalyses, and consistently with this, the precipitation amounts simulated by the model are somewhat lower than those from GPCP at this latitude.

As we saw earlier the summer cold bias of CRCM5 over the Sahara and the southern bias of the maximum surface temperature have important implications for the simulated circulations of the WAM. This also has an impact upon the vertical distribution of winds over the West Africa region,

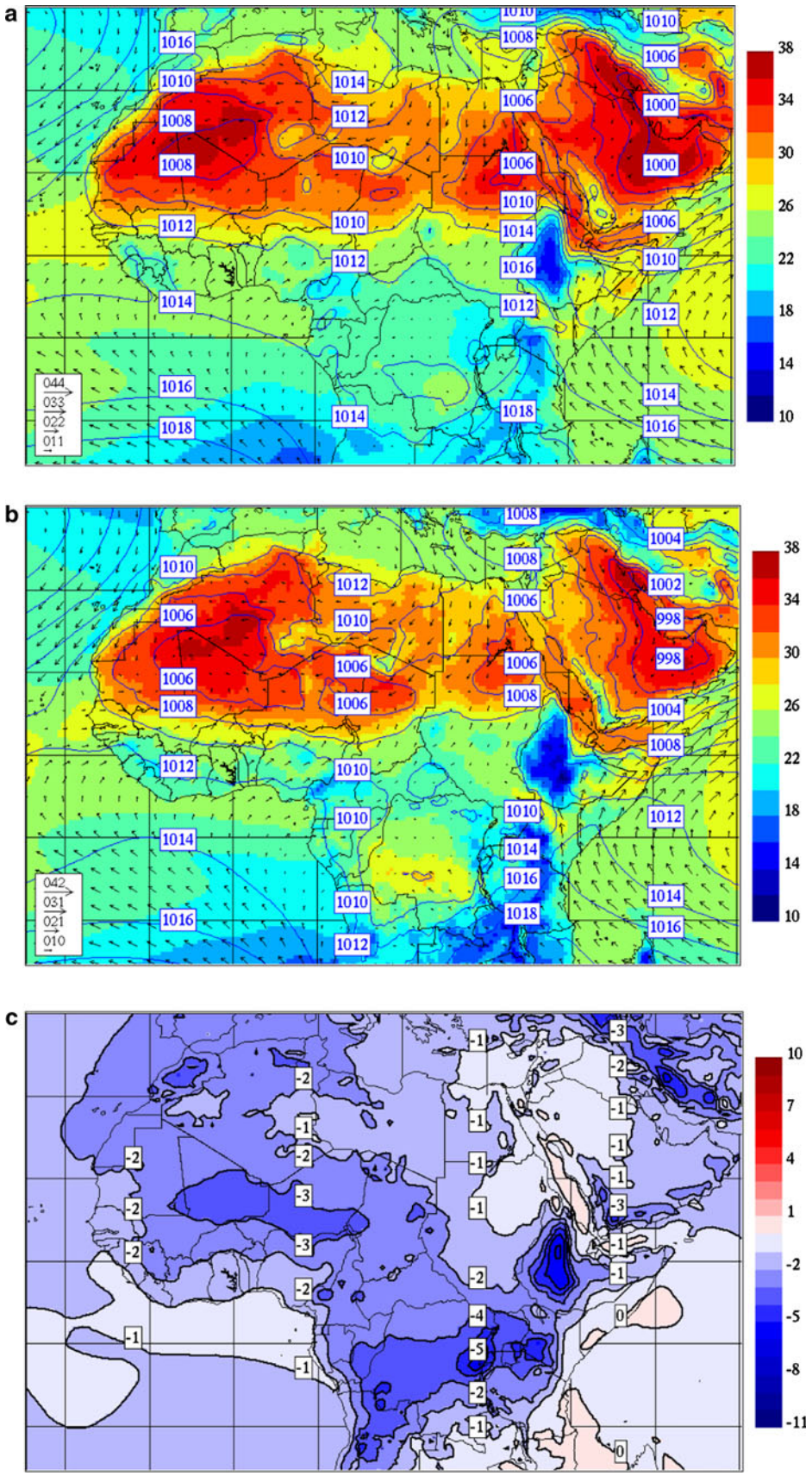

Fig. 7 Seasonal (JAS) mean (1989–2008) of **a** ERA-Interim and **b** CRCM5 fields of 2-m temperature (*colours*, °C), 925-hPa wind vectors (*arrows*, m/s) and mean sea level pressure (*contours*, hPa), and **c** the difference (CRCM5–ERA) in mean sea level pressure (*contours*, hPa)

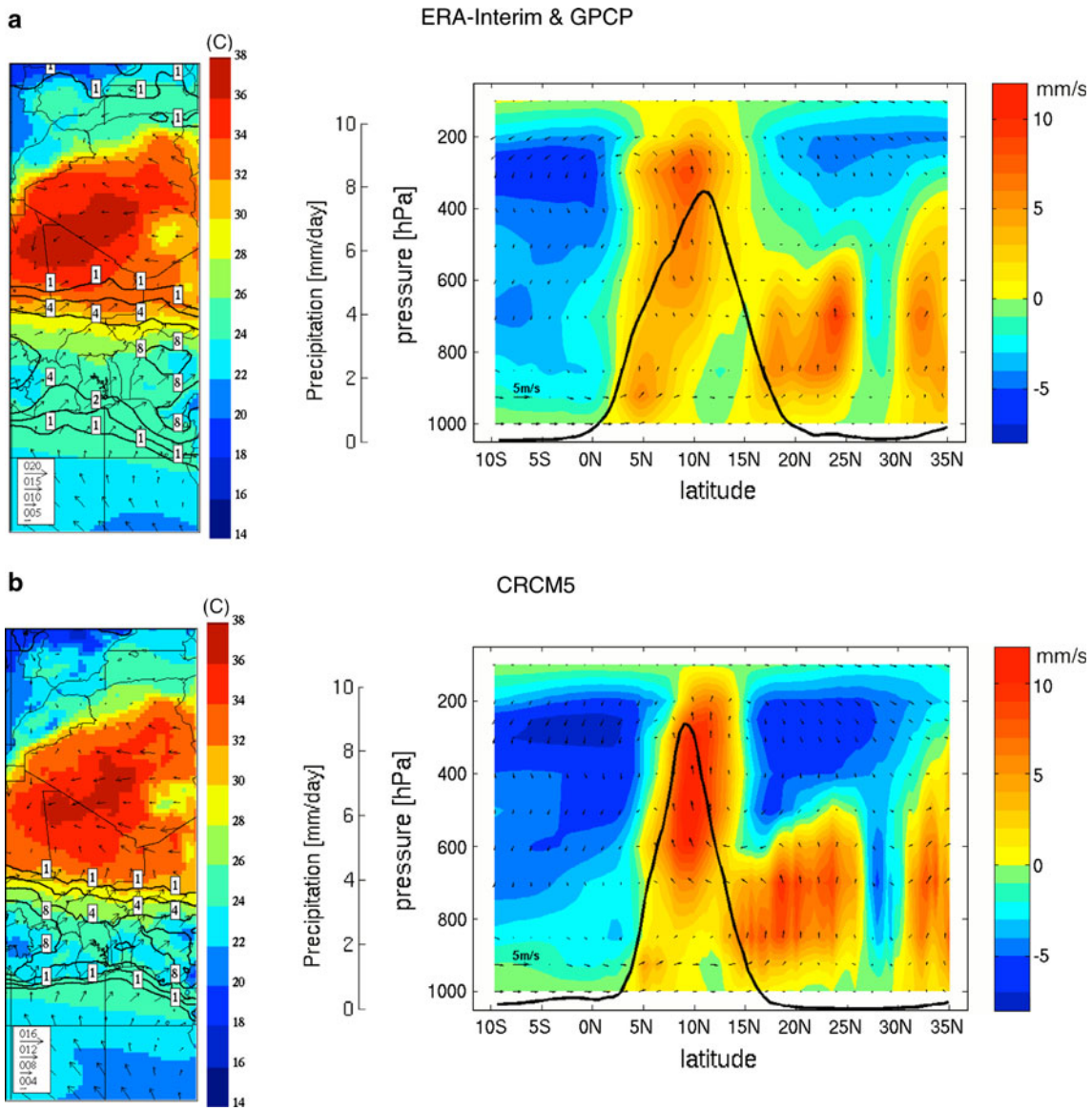

Fig. 8 *Left panels*: seasonal (JAS) mean of (*top*) ERA-Interim and (*bottom*) CRCM5 fields of 2-m temperature (*colours*, °C), 925-hPa wind vectors (*arrows*, m/s) and precipitation (mm/day). *Right panels*: Vertical cross-section as a function of latitude of seasonal (JAS) mean vertical velocity (*colours*, mm/s) and vectors combining vertical (mm/s) and meridional (m/s) velocity components (*arrows*, m/s), averaged in the region between 10°W–10°E and 10°S–35°N over the period (1997–2008), from ERA-Interim (*top*) and CRCM5 (*bottom*). Associated GPCP (*top*) and CRCM5 (*bottom*) mean precipitation (mm/day) are superimposed

as we shall see next. Figure 9 shows a vertical cross-section of the mean zonal wind in boreal summer (JAS) for the region 10°S–35°N and 10°W–10°E, top panel for ERA-Interim and bottom panel for the CRCM5 simulation. Between the surface and 850 hPa, the monsoonal and Harmattan flows appear as westerly and easterly components, respectively. At the surface, the transition occurs at 20°N in the reanalyses but further south, around 17°N, in the simulation.

Above this, in the mid-troposphere and centred around 600 hPa and 14°N, there is the African Easterly Jet (AEJ). The AEJ is a key element of the WAM circulation. It results from the strong baroclinicity between the hot and dry Sahara and the colder and humid Guinea coast, through the thermal wind relationship (Burpee 1972; Cook 1999; Thorncroft and Blackburn 1999; Parker et al. 2005a, b). There is a direct link between the divergent circulation around 600–700 hPa associated with the SMC of the SHL and the existence of the AEJ (Thorncroft and Blackburn 1999; Parker et al. 2005a). When compared to ERA-Interim, the core of the AEJ is of the right strength and almost the right height, but it is displayed southward by about 2°. At the same time, the shape of the zone of monsoonal winds is not exactly the same, with the

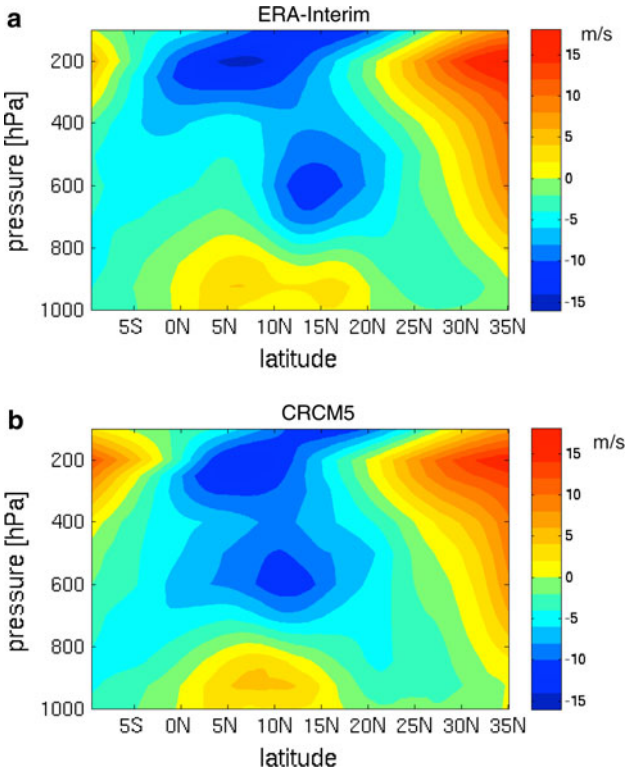

Fig. 9 Vertical cross-section of ERA-Interim (*top*) and CRCM5 (*bottom*) mean zonal wind (10°W–10°E) for the period (1989–2008)

maximum westerlies being overestimated in the model by about 2 m/s and being displaced northward: it is located at 6°N in ERA and between 5°N and 11°N in the model.

Further above, in the upper troposphere, lies the Tropical Easterly Jet (TEJ) at 200 hPa and 6°N. Compared to ERA-Interim, the core of the TEJ is slightly underestimated, by about 2 m/s; its position is correct but the shape is not exactly the same as in the reanalyses. Although in general there is an acceptable agreement between the model simulation and ERA-Interim, there are some differences in the configuration of wind distribution.

Nicholson (2008, 2009) noted that the column of rising motion associated with the tropical rainbelt is bounded to the south by the axis of the upper troposphere TEJ and to the north by the axis of the mid-troposphere AEJ. They also noted that the TEJ, which is the outflow of the Asian Monsoon, exhibits little latitudinal variations from year to year over Africa. The AEJ on the other hand can migrate south or north; a northern position of the AEJ means wet summers in the Sahel (wider tropical rainbelt) and a southern position of the AEJ implies dry summers in this region (narrower tropical rainbelt). The CRCM5 simulation appears to follow the empirical relationship established by Nicholson (2009) between the column of rising motion and the axis of the two jets. In the simulation, the axis of the AEJ is positioned close to the northern limit of the column of maximum rising motion. The model southward bias for the location of the AEJ (as is also the SHL), combined to the weakness of the TEJ, is in accordance with a deficit of rainfall in the Sahel, as noted by Nicholson (2008, 2009) in her analysis of observations. The climatology of the WAM as simulated by CRCM5 resembles the "dry Sahel" mode of the interannual variability of rainfall identified by Nicholson (2009), with a narrower column of rising motion and a southern position of the AEJ.

Interestingly enough the simulation performed by Sylla et al. (2010) using another RCM over a similar domain and at similar resolution, produced biases of opposite sign to our results. In their simulation the strength of the monsoon flow was overestimated and the location of the AEJ core was too far north compared with the reanalysis. They associated the stronger monsoon flow and northward shift of the AEJ to an overestimation of the low-level temperature gradients.

5 Discussion and conclusions

The CORDEX programme with Africa as its main target region provided the impetus for testing the new, fifth-generation Canadian Regional Climate Model (CRCM5) outside its "native" region, as recommended by the World Climate Research Programme. The African climate represents a considerable challenge due to the complexity and diversity of interacting dynamical and physical processes, in particular those contributing to the West African Monsoon (WAM) that is of paramount importance for the population under its influence.

In a 20-year simulation driven by ERA-Interim reanalyses CRCM5 successfully reproduced the overall features of geographical and seasonal temperature distribution, with seasonal mean biases generally less than $\pm 2°$ over most of the domain. The simulation also succeeded in reproducing the average distribution of precipitation and its large geographical differences, including the seasonal migration of the tropical rainbelt associated with the variations of solar declination. In particular the overall WAM is reproduced, but the simulation failed to bring the precipitation far enough north into the Sahel, which appears to be related to a weaker monsoonal flow associated to a cold bias in the Sahara. On the other hand, the simulation succeeded in reproducing fairly well the main diurnal cycle of precipitation and its geographical differences, as noted previously by Nikulin et al. (2012) in their comparison of several regional models' simulations over Africa.

Meridional cross-sections over West Africa in summer showed a good representation of the deep upward motion associated with the Hadley cell and a good representation of location and intensity of the maximum precipitation.

The low-level convergence and shallow upward motion associated with the Saharan Heat Low (SHL) is located too far south however. The African Easterly Jet (AEJ) is of the right strength and almost at the right height, but located too far to the south as a result of the displacement of the SHL.

Tests are underway to identify the underlying reasons for the cold bias in the Sahara, which are pointing towards remaining deficiencies in the attribution of surface albedo and surface emissivity over deserts. This defect may have repercussions on the simulated monsoonal flow and may in part be responsible for the summer dry bias in Sahel. The wet bias in the states of the Gulf of Guinea in summer may be related to inadequacies in the parameterisation of boundary-layer and subgrid-scale vertical transport processes.

Acknowledgments This research was funded by the Canadian Foundation for Climate and Atmospheric Sciences (CFCAS), the Québec's *Ministère du Développement Économique, Innovation et Exportation* (MDEIE), the Natural Sciences and Engineering Research Council of Canada (NSERC), Hydro-Québec, the Ouranos Consortium on Regional Climatology and Adaptation to Climate Change, the Mathematics of Information Technology and Complex Systems (MITACS) Network of Centres of Excellence, and the Canada Research Chairs programme. The calculations were made possible through an award from the Canadian Foundation for Innovation (CFI) to the CLUMEQ Consortium. The authors thank Mr. Kossivi-Yéwougni Tete for producing several figures for the final manuscript, and Mr. Georges Huard and Mrs. Nadjet Labassi for maintaining an efficient and user-friendly local computing facility. The authors are also grateful to the following collaborators at Environment Canada: Mr. Michel Desgagné for his work in developing a nested version of GEM, Dr. Diana Verseghy for allowing to use the code of CLASS 3.5, and Mr. Richard Harvey for helping with CLASS. This study would not have been possible without the access to valuable datasets such as ERA-Interim, CRU, UDEL, GPCP and TRMM.

References

Adler RF et al (2003) The version-2 Global Precipitation Climatology Project (GPCP) monthly precipitation analysis (1979-present). J Hydrometeorol 4:1147–1167

Bélair S, Mailhot J, Girard C, Vaillancourt P (2005) Boundary-layer and shallow cumulus clouds in a medium-range forecast of a large-scale weather system. Mon Weather Rev 133:1938–1960

Benoit R, Côté J, Mailhot J (1989) Inclusion of a TKE boundary layer parameterization in the Canadian regional finite-element model. Mon Weather Rev 117:1726–1750

Biner S, Caya D, Laprise R, Spacek L (2000) Nesting of RCMs by imposing large scales. In: Research activities in atmospheric and oceanic modelling. WMO/TD 987, report no. 30: 7.3–7.4

Boone A, de Rosnay P, Basalmo G, Beljaars A, Chopin F, Decharme B, Delire C, Ducharne A, Gascoin S, Grippa M, Guichard F, Gusev Y, Harris P, Jarlan L, Kergoat L, Mougin E, Nasonova O, Norgaard A, Orgeval T, Ottlé C, Poccard-Leclercq I, Polcher J, Sandholt I, Saux-Picart S, Taylor C, Xue Y (2009) The AMMA Land Surface Model Intercomparison Project. Bull Am Meteorol Soc 90:1865–1880. doi:10.1175/2009BAMS2786.1

Burpee RW (1972) The origin and structure of easterly waves in the lower troposphere of North Africa. J Atmos Sci 29:77–90

Caron L-P, Jones CG (2011) Understanding and simulating the link between African easterly waves and Atlantic tropical cyclones using a regional climate model: the role of domain size and lateral boundary conditions. Clim Dyn. doi:10.1007/s00382-011-1160-8

Caron L-P, Jones CG, Winger K (2010) Impact of resolution and downscaling technique in simulating recent Atlantic tropical cyclone activity. Clim Dyn. doi:10.1007/s00382-010-0846-7

Cook KH (1999) Generation of the African easterly jet and its role in determining West African precipitation. J Clim 12:1165–1184

Côté J, Gravel S, Méthot A, Patoine A, Roch M, Staniforth A (1998a) The operational CMC-MRB global environmental multiscale (GEM) model. Part I: design considerations and formulation. Mon Weather Rev 126:1373–1395

Côté J, Desmarais JG, Gravel S, Méthot A, Patoine A, Roch M, Staniforth A (1998b) The operational CMC-MRB global environmental multiscale (GEM) model. Part II: results. Mon Weather Rev 126:1397–1418

Dai A, Lin X, Hsu K-L (2007) The frequency, intensity, and diurnal cycle of precipitation in surface and satellite observations over low- and mid-latitudes. Clim Dyn 29:727–744. doi:10/1007/s00382-007-0260-y

Davies HC (1976) A lateral boundary formulation for multi-level prediction models. QJR Meteorol Soc 102:405–418

Delage Y (1997) Parameterising sub-grid scale vertical transport in atmospheric models under statically stable conditions. Bound Layer Meteorol 82:23–48

Delage Y, Girard C (1992) Stability functions correct at the free convection limit and consistent for both the surface and Ekman layers. Bound Layer Meteorol 58:19–31

Diaconescu EP, Laprise R, Zadra A (2011) Singular vector decomposition of the internal variability of the Canadian regional climate. Clim Dyn. doi:10.1007/s00382-011-1179-x

Druyan LM (2010) Studies of the 21st century precipitation trends over West Africa. Int J Climatol. doi:10.1002/joc.2180

Druyan LM, Feng J, Cook KH, Xue Y, Fulakeza M et al (2010) The WAMME regional model intercomparison study. Clim Dyn 35:175–192

Fox-Rabinovitz M, Côté J, Dugas B, Déqué M, McGregor JL (2006) Variable resolution general circulation models: stretched-grid model intercomparison project (SGMIP). J Geophys Res 111:D16104. doi:10.1029/2005JD006520

Giorgi F, Jones C, Asrar G (2009) Addressing climate information needs at the regional level: the CORDEX framework. World Meteorol Organ Bull 58:175–183. Available online at http://wcrp.ipsl.jussieu.fr/RCD_Projects/CORDEX/CORDEX_giorgi_WMO.pdf

He Y, Monahan AH, Jones CG, Dai A, Biner S, Caya D, Winger K (2010) The probability distribution of land surface wind speed over North America. J Geophys Res Atmos 115:D04103. doi:10.1029/2008JD010708

Hodges KI, Thorncroft CD (1997) Distribution and statistics of African mesoscale convective weather systems based on the ISCCP Meteosat imagery. Mon Weather Rev 125:2821–2837

Hourdin F, Guichard F, Favot F, Marquet P, Boone A, Lafore JP, Redelsperger JL, Ruti P, Dell'Aquila A, Doval TL, Traore AK, Gallee H (2010) AMMA-model intercomparison project. Bull Am Meteorol Soc 1:95–104

Huffman GJ, Adler RF, Morrissey MM, Bolvin DT, Curtis S, Joyce R, McGavock B, Susskind J (2001) Global precipitation at one-

degree daily resolution from multisatellite observations. J Hydrometeor 2:36–50
Huffman GJ, Adler RF, Bolvin DT, Gu G, Nelkin EJ, Bowman KP, Stocker EF, Wolff DB (2007) The TRMM multi-satellite precipitation analysis: quasi-global, multi-year, combined-sensor precipitation estimates at fine scale. J Hydrometeor 8:33–55
IPCC AR4 (2007) Climate change 2007: the physical science basis. Contribution of working group I (WGI) to the fourth assessment report (AR4) of the Intergovernmental Panel on Climate Change (IPCC) [Solomon S, Qin D, Manning M, Chen Z, Marquis M, Averyt KB, Tignor M, Miller HL (Eds)]. Cambridge University Press, Cambridge. http://www.ipcc.ch/publications_and_data/ar4/wg1/en/contents.html
Kain JS, Fritsch JM (1990) A one-dimensional entraining/detraining plume model and application in convective parameterization. J Atmos Sci 47:2784–2802
Kuo HL (1965) On formation and intensification of tropical cyclones through latent heat release by cumulus convection. J Atmos Sci 22:40–63
Laprise R (1992) The Euler equation of motion with hydrostatic pressure as independent coordinate. Mon Weather Rev 120:197–207
Laprise R (2008) Regional climate modelling. J Comp Phys 227:3641–
3666
Lavaysse C, Flamant C, Janicot S, Parker DJ, Lafore JP, Sultan B, Pelon J (2009) Seasonal evolution of the West African heat low: a climatological perspective. Clim Dyn 33:313–330
Lebel T, Cappelaere B, Galle S, Hanan N, Kergoat L, Levis S, Vieux B, Descroix L, Gosset M, Mougin E, Peugeot Ch, Seguis L (2009) AMMA-CATCH studies in the Sahelian region of West-Africa: an overview. J Hydrol 375:3–13
Legates DR, Willmott CJ (1990a) Mean seasonal and spatial variability global surface air temperature. Theoret Appl Climatol 41:11–21
Legates DR, Willmott CJ (1990b) Mean seasonal and spatial variability in gauge-corrected, global precipitation. Int J Climatol 10:111–127
Li J, Barker HW (2005) A radiation algorithm with correlated-k distribution. Part I: local thermal equilibrium. J Atmos Sci 62:286–309
Martynov A, Sushama L, Laprise R (2010) Simulation of temperate freezing lakes by one-dimensional lake models: performance assessment for interactive coupling with regional climate models. Boreal Environ Res 15:143–164 (ISSN 1797-2469 online; ISSN 1239-6095 print, 2010)
Martynov A, Sushama L, Laprise R, Winger K, Dugas B (2012) Interactive lakes in the Canadian regional climate model, version 5: the role of lakes in the regional climate of North America. Tellus A 64:16226–16245. doi:10.3402/tellusa.v64i0.16226
Masson V, Champeaux J-L, Chauvin F, Meriguet Ch, Lacaze R (2003) A global database of land surface parameters at 1-km resolution in meteorological and climate models. J Clim 16:1261–1282 (data available online at http://www.cnrm.meteo.fr/gmme/PROJETS/ECOCLIMAP/page_ecoclimap.htm)
McFarlane NA (1987) The effect of orographically excited gravity-wave drag on the general circulation of the lower stratosphere and troposphere. J Atmos Sci 44:1775–1800
McGarry MM, Reed RJ (1978) Diurnal variations in convective activity and precipitation during phases II and III of GATE. Mon Weather Rev 106:101–113
Mitchell TD, Jones PD (2005) An improved method of constructing a database of monthly climate observations and associated high-resolution grids. Int J Climatol 25:693–712
Mitchell TD, Carter TR, Jones PD, Hulme M, New M (2004) A comprehensive set of high-resolution grids of monthly climate for Europe and the globe: the observed record (1901–2000) and 16 scenarios (2001–2100). Tyndall Centre for Climate Change Research, Norwich, working paper 55. Available online at http://www.cru.uea.ac.uk/
Nicholson SE (2008) The intensity, location and structure of the tropical rainbelt over West Africa as factors in interannual variability. Int J Climatol 28:1775–1785
Nicholson SE (2009) A revised picture of the structure of the "monsoon" and land ITCZ over West Africa. Clim Dyn 32:1155–1171
Nikulin G, Jones C, Giorgi F, Asrar G, Büchner M, Cerezo-Mota R, Christensen OB, Déqué M, Fernandez J, Hänsler A, van Meijgaard E, Samuelsson P, Sylla MB, Sushama L (2012) Precipitation climatology in an ensemble of CORDEX-Africa regional climate simulations. J Clim. doi:10.1175/JCLI-D-11-00375.1
Paeth H, Hall Nicholas MJ, Gaertner MA, Dominguez Alonso M, Moumouni S, Polcher J, Ruti PM, Fink AH, Gosset M, Lebel T, Gaye AT, Rowell DP, Moufouma-Okia W, Jacob D, Rockel B, Giorgi F, Rummukainen M (2011) Progress in regional downscaling of West Africa precipitation. Atmos Sci Let 12:75–82
Paquin-Ricard D, Jones C, Vaillancourt PA (2010) Using ARM observations to evaluate cloud and clear-sky radiation processes as simulated by the Canadian regional climate model GEM. Mon Weather Rev 138:818–838
Parker DJ, Burton RR, Diongue-Niang A et al (2005a) The diurnal cycle of the West African monsoon circulation. QJR Meteorol Soc 131:2839–2860
Parker DJ, Thorncroft CD, Burton RR, Diongue-Niang A et al (2005b) Analysis of the African Easterly Jet using aircraft observations from the JET2000 experiment. QJR Meteorol Soc 131:1461–1482
Ploshay JJ, Lau N-C (2010) Simulation of the diurnal cycle in tropical rainfall and circulation during boreal summer with a high-resolution GCM. Mon Weather Rev 138:3434–3453
Redelsperger JL, Thorncroft CD, Diedhiou A, Lebel T, Parker DJ, Polcher J (2006) African monsoon multidisciplinary analysis: an international research project and field campaign. Bull Am Meteorol Soc 87:1739–1746
Riette S, Caya D (2002) Sensitivity of short simulations to the various parameters in the new CRCM spectral nudging. Research activities in Atmospheric and Oceanic Modelling, edited by H. Ritchie, WMO/TD—no 1105, report no. 32:7.39–7.40
Šeparović L, de Elía R, Laprise R (2011) Impact of spectral nudging and domain size in studies of RCM response to parameter modification. Clim Dyn. doi: 10.1007/s00382-011-1072-7
Simmons AS, Uppala DD, Kobayashi S (2007) ERA-interim: new ECMWF reanalysis products from 1989 onwards. ECMWF Newslett 110:29–35
Sundqvist H, Berge E, Kristjansson JE (1989) Condensation and cloud parameterization studies with a mesoscale numerical weather prediction model. Mon Weather Rev 117:1641–1657
Sylla MB, Coppola E, Mariotti L, Giorgi F, Ruti PM, Dell'Aquila A, Bi X (2010) Multiyear simulation of the African climate using a regional climate model (RegCM3) with the high resolution ERA-Interim reanalysis. Clim Dyn 35:231–247. doi: 10.1007/s00382-009-0613-9
Takle ES, Roads J, Rockel B, Gutowski WJ Jr, Arritt RW, Meinke I, Jones CG, Zadra A (2007) Transferability intercomparison: an opportunity for new insight on the global water cycle and energy budget. Bull Am Meteorol Soc 88:375–384
Tanguay M, Yakimiv E, Ritchie H, Robert A (1992) Advantages of spatial averaging in semi-implicit semi-Lagrangian schemes. Mon Weather Rev 120:115–123
Thorncroft CD, Blackburn M (1999) Maintenance of the African easterly jet. QJR Meteorol Soc 125:763–786

Thorncroft CD, Nguyen H, Zhang C, Peyrillé P (2011) Annual cycle of the West African monsoon: regional circulations and associated water vapour transport. QJR Meteorol Soc 137:129–147. doi:10.1002/qj.728

Uppala S, Dee D, Kobayashi S, Berrisford P, Simmons A (2008) Towards a climate data assimilation system: status update of ERA-interim. ECMWF Newslett 115:12–18

Verseghy LD (2000) The Canadian land surface scheme (CLASS): its history and future. Atmos Ocean 38:1–13

Verseghy LD (2008) The Canadian land surface scheme: technical documentation—version 3.4. Climate Research Division, Science and Technology Branch, Environment Canada

Willmott CJ, Matsuura K, Legates DR (1998) Global air temperature and precipitation: regridded monthly and annual climatologies (version 2.01). Available online at: http://climate.geog.udel.edu/∼climate/

Xue Y, De Sales F, Lau WKM, Boone A, Feng J et al (2010) Intercomparison and analyses of the climatology of the West African Monsoon in the West African Monsoon Modeling and Evaluation project (WAMME) first model intercomparison experiment. Clim Dyn 35:3–27

Yang GY, Slingo J (2001) The diurnal cycle in the Tropics. Mon Weather Rev 129:784–801

Yeh KS, Gravel S, Méthot A, Patoine A, Roch M, Staniforth A (2002) The operational CMC-MRB global environmental multiscale (GEM) model. Part III: non-hydrostatic formulation. Mon Weather Rev 130:339–356

Zadra A, Roch M, Laroche S, Charron M (2003) The subgrid scale orographic blocking parameterization of the GEM model. Atmos Ocean 41:155–170

Zadra A, Caya D, Côté J, Dugas B, Jones C, Laprise R, Winger K, Caron LPh (2008) The next Canadian regional climate model. Phys Canada 64:75–83